Prostate Brachytherapy Seed Reconstruction Using C-Arm Rotation Measurement and Motion Compensation*

Ehsan Dehghan[1], Junghoon Lee[2], Mehdi Moradi[3], Xu Wen[3], Gabor Fichtinger[1], and Septimiu E. Salcudean[3]

[1] Queen's University, Canada
[2] Johns Hopkins University, USA
[3] University of British Columbia, Canada

Abstract. During prostate brachytherapy, C-arm flouroscopy images are used for a qualitative assessment of the procedure. Three dimensional reconstruction of the implanted seeds can be used for intraoperative dosimetry and quantitative assessment. Accurate C-arm pose estimation is necessary for 3D localization of the seeds. We propose to measure the C-arm rotation angles and computationally compensate the inevitable C-arm translational motion to estimate the pose. We compensate the oscillation, sagging and wheel motion of the C-arm using a three-level optimization algorithm, without which the reconstruction can fail. We validated our approach on simulated and 10 data sets from 5 patients and gained on average 99.1% success rate, 0.33 mm projection error and computation time of less than one minute per patient, which are clinically excellent results.

1 Introduction

Low dose rate prostate brachytherapy is an effective treatment for localized prostate cancer which entails permanent placement of radio-active capsules or "seeds" inside the prostate. The seeds are delivered to preoperatively determined positions using needles under real-time visual guidance from ultrasound. The quality of the treatment depends on the accurate placement of the seeds to deliver sufficient radiation to the cancer while sparing the healthy tissue. However, seed misplacements and consequent complications are common. C-arm fluoroscopy images are taken during the procedure to visually assess the implant (see Fig. 1(a)). Three dimensional reconstruction of the seeds has several benefits such as intraoperative dosimetry modifications and quantitative assessment, and has been proposed previously [1,2,3].

Seed reconstruction entails solving a seed matching problem – assigning the shadows of a seed in different images to each other- which has been solved using simulated annealing [1], Hungarian algorithm [2] and linear programing [3].

* This work was supported by an Ontario Ministry of Research and Innovation postdoctoral fellowship and NIH R21CA120232-01. The authors are grateful to Dr. W. J. Morris from British Columbia Cancer Agency for providing the clinical data.

T. Jiang et al. (Eds.): MICCAI 2010, Part I, LNCS 6361, pp. 283–290, 2010.

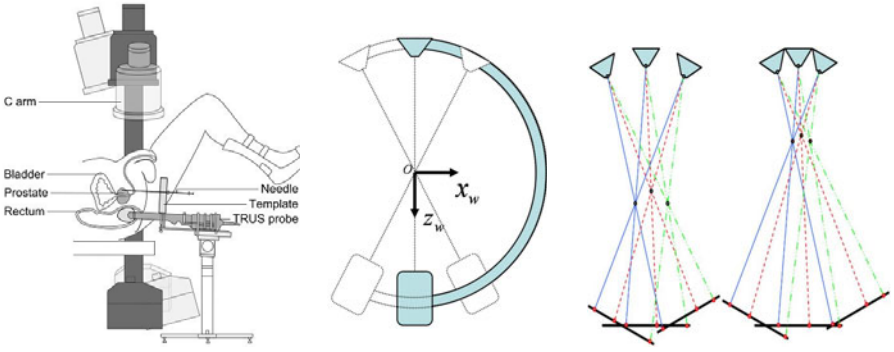

Fig. 1. (a) Brachytherapy procedure, (b) rotation of the C-arm around the primary axis (PA) and the world coordinate system, and (c) the scaling problem. In (c), the left C-arms have the same intrinsic parameters, rotation angles, X-ray images, reconstruction cost and matching as the right ones; however, the seed cloud is scaled.

Seed matching and reconstruction are performed using known C-arm pose, estimated using radio-opaque beads or fiducials [4,5,6], or obtained from optical and electromagnetic trackers [7]. The fiducials and beads may interfere with the anatomy in the images, require segmentation and can limit the clinical working volume. Auxiliary trackers are expensive and further complicate the surgery as they need calibration steps, line of sight and space in the operating room. It has been suggested that implanted seeds can be used for pose estimation [1,8]. However, to be computationally feasible, they need an initial estimation of the pose, conveniently by using external trackers and fiducials.

If C-arm images are taken by rotation of the C-arm around a fixed axis (see Fig. 1(b)), known rotation angles will yield the relative pose. C-arm devices are available with or can be easily equipped with a joint encoder. A simple digital protractor can also be used to measure the C-arm angles. However, oscillation and sagging of the C-arm, especially in the elevational direction are significant due to the C-arm weight. The movements in the two other perpendicular directions caused by wheel motion are much smaller but are often significant. If unattended, C-arm translational movements cause inaccuracies in the pose estimation which may lead to reconstruction failure.

We demonstrate that in the case of a C-arm with small angle span around a single axis, sole measurement of rotation angles combined with a computational algorithm to compensate for C-arm oscillation, sagging and wheel motion suffices for a successful and accurate reconstruction. However, the reconstruction is prone to failure without such a motion compensation. By measuring the angles using joint encoders or protractors, we obviate the need for full pose tracking using fiducials or external trackers. Considering the simplicity of the implementation, high speed and accuracy of reconstruction, this approach is especially suitable for clinical translation.

2 Methods

In order to solve the matching problem, we rely on a linear programing approach introduced by Lee *et al.* [3] which, for sake of completeness, we outline in Section 2.1. The motion compensation method is discussed in detail in Section 2.2.

2.1 Seed Localization Using Linear Programing

Assume that three projection images of N implanted seeds are available and $N_i, i \in \{1,2,3\}$ seed shadows are segmented in each image. The matching problem can then be written as:

$$\min_{x_{ijk}} \sum_{i=1}^{N_1} \sum_{j=1}^{N_2} \sum_{k=1}^{N_3} c_{ijk} x_{ijk},$$
$$\text{s.t.} \begin{cases} \sum_{j=1}^{N_2} \sum_{k=1}^{N_3} x_{ijk} \geq 1, & \forall i \\ \sum_{i=1}^{N_1} \sum_{k=1}^{N_3} x_{ijk} \geq 1, & \forall j \\ \sum_{i=1}^{N_1} \sum_{j=1}^{N_2} x_{ijk} \geq 1, & \forall k \\ \sum_{i=1}^{N_1} \sum_{j=1}^{N_2} \sum_{k=1}^{N_3} x_{ijk} = N, \\ x_{ijk} \in \{0,1\}, \end{cases} \tag{1}$$

where c_{ijk} is the cost of matching seed shadows p_i^1, p_j^2 and p_k^3 from the first, second and third images, respectively, and x_{ijk} is a binary variable showing the correctness of such an assignment. The cost c_{ijk} is the symbolic distance between lines L_i^1, L_j^2 and L_k^3 which connect the seed shadows p_i^1, p_j^2 and p_k^3 to their corresponding X-ray source locations in 3D space. Equation (1) can be written as a constrained linear programing problem by concatenating the x_{ijk} and c_{ijk} into vectors. The unknowns that correspond to a cost higher than a specified threshold are removed and the linear programing problem with reduced dimensions is solved to find the correct seed matching solution [3].

2.2 Motion Compensation Algorithm

It has been shown that higher accuracy in C-arm pose estimation will result in more accurate matching and vice versa [1,8]. Therefore, the matching and the motion compensation problems can be solved iteratively in a loop in which reconstructed seed positions can be used to improve on C-arm pose estimation.

Assume a world coordinate system $Ox_w y_w z_w$ centered at the center of rotation of the C-arm, with unit vectors x_w and z_w as shown in Fig. 1(b) and y_w perpendicular to the plane of rotation and aligned with the craniocaudal axis of the patient. The coordinates of the X-ray source corresponding to image i are q_i in $Ox_w y_w z_w$. Measured rotation angles and known intrinsic parameters, such as focal length and source to center distance, yield good initial estimates for q_i and the corresponding pose.

The goal of our motion compensation algorithm is to find the optimal position adjustments (offsets) δ_n for the source positions to solve the following problem:

$$\min_{x_{ijk}, \delta_n} \sum_{i=1}^{N_1} \sum_{j=1}^{N_2} \sum_{k=1}^{N_3} c_{ijk}(\delta_n) x_{ijk}, \quad n \in \{1,2,3\}, \tag{2}$$

subject to the constraints from Eq. (1).

In order to compensate the motion of the C-arm, one may try to find the positions of the source corresponding to the second and third images (henceforth called second and third source positions) relative to the position of the source corresponding to the first image (henceforth, the first source position). It is known that this problem can be solved in 3D up to a scale [1,8], which means that the reconstructed volume can arbitrary shrink or expand (see Fig 1(c)). In [8], the distance between two points on a radio-opaque fiducial was used to find the scaling factor. However, we do not use an external fiducial here.

Through observation, it can be seen that C-arm motion along x_w is less significant compared to the motion along y_w and especially z_w, along which we expect the largest motion. In order to avoid the scaling problem, we will constrain the C-arm motion to the Oy_wz_w plane.

First-Level Optimization: In the first level of optimization, we find matching seeds in the images to provide an initial offset estimate. Since the fluoroscopy images are generally taken by rotation of the C-arm around the y_w axis only, the seeds located at the top or at the bottom of one image appear at the top or at the bottom of other images. We use this observation and select $n = 5$ seed shadows from the top and n seeds from the bottom of the images and solve the matching problem for them. Since these n seed shadows do not necessarily correspond to n seeds in 3D, the matching problem is solved as in Eq. (1), while the fourth constraint is relaxed. We fix the first source in 3D space and optimize the 2D offsets (to avoid scaling) for the other two sources to minimize the overall reconstruction cost for $p = 4$ seeds (2 from the top and 2 from the bottom of the image) which have the least reconstruction cost. The matching and the 2D offset calculation are iteratively solved until there is no change in the matching.

Second-Level Optimization: At first, seed matching is solved with the given 2D offset parameters from the first level and the 3D positions of the seeds are calculated. Then, the positions of the three sources are adjusted in 3D space to minimize the reconstruction error for the given 3D seeds. The matching and source position adjustments are iteratively performed until either the reconstruction cost or the change in the reconstruction cost between two iterations is less than an empirically assigned threshold ($<$0.1 mm for the former and $<$0.1% for the latter). The 3D position of source i at iteration $(k+1)$ is calculated as:

$$q_i^{k+1} = \left(\sum_{j=1}^{N} (I - v_{ij} v'_{ij}) \right)^{-1} \sum_{j=1}^{N} (I - v_{ij} v'_{ij}) s_j^k, \tag{3}$$

where, s_j^k is the position of the j^{th} seed at iteration k, v_{ij} is the unit vector from the source q_i^k to the shadow of seed j on image i, and I is a 3×3 identity matrix.

Since in each iteration, the position of the seeds in 3D space is fixed, the shrinkage or expansion is very small. However, as the algorithm iterates the scaling factor can become significant. It should be noted that the matching problem has a solution independent of the scaling factor (see Fig 1(c)). Therefore,

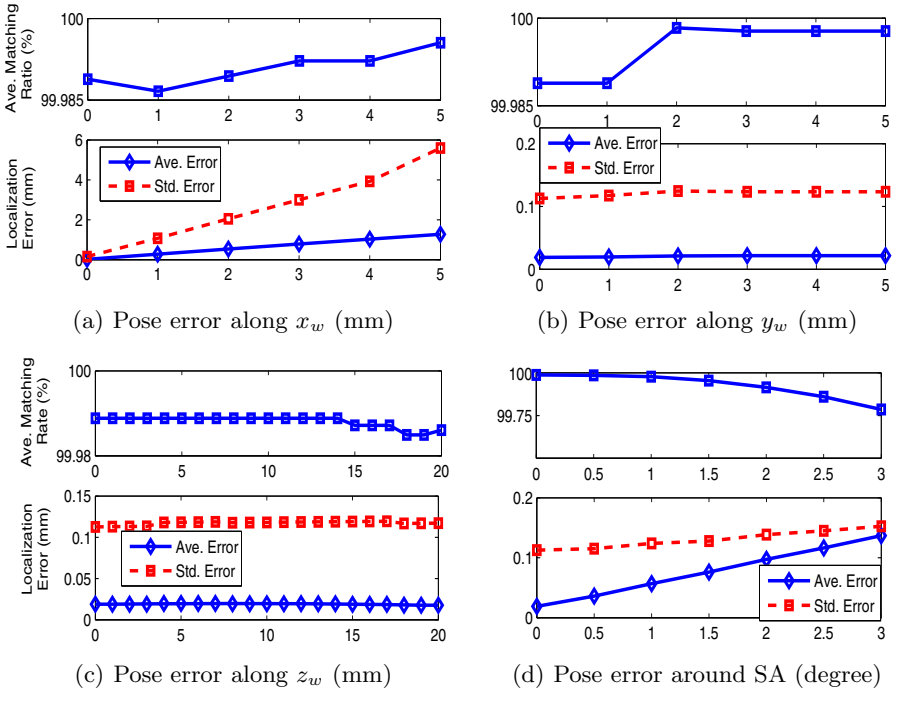

(a) Pose error along x_w (mm)

(b) Pose error along y_w (mm)

(c) Pose error along z_w (mm)

(d) Pose error around SA (degree)

Fig. 2. Simulation results, showing the matching ratio and localization error for variable pose errors

we exploit the advantages of a 3D motion compensation in this level to increase the likelihood of finding the correct matching.

Third-Level Optimization: At this point in the workflow, the correct matching is available, but seed positions may be scaled as a result of 3D motion compensation. In the third level, once more, we assume that pose error along x_w is negligible. The source positions are initialized at their ideal positions, using the rotation angle readings and C-arm's intrinsic parameters. Then, the 2D offset parameters are calculated, assuming that the first source is fixed. Note that we are only interested in the relative positions of the seeds, since the seed cloud will be registered to the prostate anatomy.

3 Results and Discussion

First, the motion compensation algorithm was tested on simulated data. We synthesized 3D positions of seeds, based on realistic dosimetry plans of four patients with 100, 108, 110 and 130 seeds. The seed shadows were simulated by rotating the C-arm around the primary axis (PA) at 0°, ±5° and ±10° while keeping

the secondary axis (SA) fixed at 180°. The seed locations were reconstructed for every combination of three images out of the available five for each patient, while translational and rotational errors were added to the third C-arm pose in each set. The added pose error was 0-5 mm along x_w and y_w, 0-20 mm along z_w and 0-3 degrees around SA. There were on average 1.6 hidden seeds per image with a maximum of 14. The reconstructed seeds were compared against the ground truth in term of localization errors, defined as the distance between the true and reconstructed seed positions after a rigid rotation and translation of the reconstructed seed cloud. The average matching ratio and localization error are shown in Fig. 2. As it can be seen the reconstruction algorithm shows consistently successful performance over a wide range of C-arm translational position errors, while the performance without motion compensation decreases with measurement errors [3]. It can be seen in Figs. 2(b) and 2(c) that the localization error and the matching ratio are almost constant for the errors added along z_w and y_w, since we compensated the motion along these two directions. The matching ratio for pose error along x_w is almost constant as shown in Fig. 2(a), since the second-level optimization finds the correct matching using a 3D offset optimization. However, since a 2D optimization is used in the third level, the localization error increases with the pose error along x_w. As expected, the localization and matching errors increase with the measurement error around SA. However, the matching ratio remains well above clinically acceptable threshold, which is customarily around 98%.

The motion compensation algorithm was also tested on patient data. Five patients were chosen with implanted ^{125}I seeds. Five images were taken for each patient at angles approximately 0°, ±5° and ±10° around y_w. Accurate rotation angles were measured using a digital protractor attached to the C-arm, which does not interfere with the image or the working space. The images were taken using a GE OEC® 9800 with motorized joints. This particular C-arm is a solid machine with a fixed axis of rotation. However, it has a heavy intensifier which makes sagging problem more severe. The rotation around the SA was set to be constant; however, a variation of 1° was observed according to the C-arm joint angle readings and was taken into account during seed reconstruction. We reconstructed the seeds using manually segmented images taken at $(0°, \pm 5°)$ and $(0°, \pm 10°)$ for each patient (10 data sets in total). There were an average of 1.45 and maximum of 6 hidden seeds in the images. We assumed that the C-arm intrinsic parameters do not change due to small span of rotation. After reconstruction the seeds were projected on the images. Projection error, measured as the distance of the centroid of the seed and the projected location of the seed is reported in Table 1. Figure 3 is a sample of projected seeds on an image, showing very small errors. The images were meticulously inspected to detect any mismatching of seeds. The matching success rate and the reconstruction time are reported in Table 1. In the second data set of the third patient, 8 seeds showed ambiguous assignments and were conservatively considered as mismatches. Therefore, the reported matching ratio is smaller or equal to the real matching ratio.

Table 1. Clinical results."F" stands for reconstruction failure

Patient Number	Number of seeds	App. Angles (degree)	Match rate	Ave. Proj. Err. (mm)	Std. Proj. Err. (mm)	Comp. time(s)	Match rate w/o MC
1	105	$(0, \pm 5)$	100%	0.32	0.20	45	<95%
		$(0, \pm 10)$	100%	0.37	0.25	53	F
2	102	$(0, \pm 5)$	100%	0.22	0.12	32	<97%
		$(0, \pm 10)$	100%	0.31	0.18	39	F
3	100	$(0, \pm 5)$	100%	0.31	0.19	43	F
		$(0, \pm 10)$	92%	0.32	0.19	57	F
4	115	$(0, \pm 5)$	99.1%	0.51	0.28	60	<90%
		$(0, \pm 10)$	100%	0.33	0.22	28	F
5	113	$(0, \pm 5)$	100%	0.23	0.18	48	97.3%
		$(0, \pm 10)$	100%	0.36	0.23	56	F

The reconstruction ratio without motion compensation is also reported in Table 1. Reconstructions with a success rate smaller than 80% are considered as failure. As it can be seen, in 6 out of 10 data sets the reconstruction without motion compensation failed, and in the remaining 4 cases the matching ratio was considerably lower than with motion compensation (the projection error was significantly larger and is not reported here). Comparison of the reconstruction results with and without motion compensation proves the necessity of motion compensation when only the C-arm joint angles are measured.

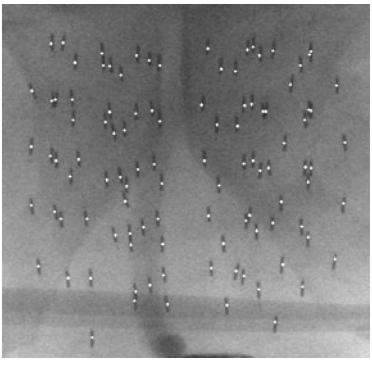

Fig. 3. Projected seeds overlaid on a C-arm fluoroscopy image

The algorithm was implemented using MATLAB on a PC with an Intel 2.33 GHz Core2 Quad CPU and 3.25 GB of RAM. The first-level optimization is fast as we select in total 10 seeds from each image. The second level is the most time consuming part of the algorithm since the seed matching problem should be solved for several iterations. The seed matching problem can be solved in approximately 10 s or less per iteration, depending on the number of seeds. The second-level optimization never took more than 10 iterations both in the simulations and patient study. The initial 2D offsets from the first level decrease the number of necessary iterations in the second level, that in turn decreases the overall computational time. The third level has a closed form solution and can be solved very fast. The motion compensation and seed reconstruction took less than one minute for each clinical case. Detailed clinical study with additional patient data is in progress.

4 Conclusion and Future Work

In conclusion, we introduced a motion compensation algorithm that combined with C-arm joint angle measurement can be used to estimate the C-arm pose for brachytherapy seed reconstruction. For joint angle measurement an off-the-shelf digital protractor was used. This removed the need for full pose tracking with fiducials or external trackers. The clinical study showed the feasibility of the method to be used in the operating room. With an average matching ratio above 99.1%, average projection error of less than 0.33 mm and a computation time less than one minute, the algorithm is suitable for clinical application.

The optimization on the third degree of freedom was ignored to avoid the scaling effect. Investigation on using the length of a ^{125}I seed to find the scaling factor and compensate the motion in 3D is part of the future work. The seeds were segmented manually. The effects of segmentation errors and application of automatic segmentation methods (e.g. [9]) will be inspected in the future.

References

1. Tubic, D., Zaccarin, A., Beaulieu, L., Pouliot, J.: Automated seed detection and three-dimensional reconstruction. II. Reconstruction of permanent prostate implants using simulated annealing. Medical Physics 28(11), 2272–2279 (2001)
2. Jain, A.K., Zhou, Y., Mustufa, T., Burdette, E.C., Chirikjian, G.S., Fichtinger, G.: Matching and reconstruction of brachytherapy seeds using the Hungarian algorithm (MARSHAL). Medical Physics 32, 3475–3492 (2005)
3. Lee, J., Labat, C., Jain, A.K., Song, D.Y., Burdette, E.C., Fichtinger, G., Prince, J.L.: Optimal matching for prostate brachytherapy seed localization with dimension reduction. In: Yang, G.-Z., Hawkes, D., Rueckert, D., Noble, A., Taylor, C. (eds.) MICCAI 2009. LNCS, vol. 5761, pp. 59–66. Springer, Heidelberg (2009)
4. Navab, N., Bani-Hashemi, A., Mitschke, M., Holdsworth, D.W., Fahrig, R., Fox, A.J., Graumann, R.: Dynamic geometrical calibration for 3-D cerebral angiography. In: SPIE Medical Imaging, vol. 2708, pp. 361–370 (1996)
5. Brack, C., Gotte, H., Gosse, F., Moctezuma, J., Roth, M., Schweikard, A.: Towards accurate X-ray camera calibration in computer-assisted robotic surgery. In: Proc. Int. symp. Computer Assisted Radiology, pp. 721–728 (1996)
6. Jain, A.K., Mustafa, T., Zhou, Y., Burdette, C., Chirikjian, G.S., Fichtinger, G.: FTRAC – A robust fluoroscope tracking fiducial. Medical Physics 32(10), 3185–3198 (2005)
7. Peters, T., Cleary, K. (eds.): Image-Guided Interventions: Technology and Applications. Springer, Heidelberg (2008)
8. Jain, A., Fichtinger, G.: C-arm tracking and reconstruction without an external tracker. In: Larsen, R., Nielsen, M., Sporring, J. (eds.) MICCAI 2006. LNCS, vol. 4190, pp. 494–502. Springer, Heidelberg (2006)
9. Lam, S.T., Marks II, R.J., Cho, P.S.: Prostate brachytherapy seed segmentation using spoke transform. In: Proc. SPIE., vol. 4322, pp. 1490–1500 (2001)